Proteomics 2014, *14*, 1107–1115 DOI 10.1002/pmic.201300422

RESEARCH ARTICLE

Spike-in SILAC proteomic approach reveals the vitronectin as an early molecular signature of liver fibrosis in hepatitis C infections with hepatic iron overload

Claudia Montaldo[1,2], Simone Mattei[1], Andrea Baiocchini[2], Nicolina Rotiroti[2], Franca Del Nonno[2], Leopoldo Paolo Pucillo[2], Angela Maria Cozzolino[1], Cecilia Battistelli[1], Laura Amicone[1], Giuseppe Ippolito[2], Vera van Noort[3], Alice Conigliaro[1], Tonino Alonzi[2], Marco Tripodi[1,2] and Carmine Mancone[1,2]*

[1] Department of Cellular Biotechnologies and Haematology, Istituto Pasteur-Fondazione Cenci Bolognetti, Sapienza University of Rome, Italy
[2] "L. Spallanzani" National Institute for Infectious Diseases, IRCCS, Rome, Italy
[3] European Molecular Biology Laboratory, Heidelberg, Germany

Hepatitis C virus (HCV)-induced iron overload has been shown to promote liver fibrosis, steatosis, and hepatocellular carcinoma. The zonal-restricted histological distribution of pathological iron deposits has hampered the attempt to perform large-scale in vivo molecular investigations on the comorbidity between iron and HCV. Diagnostic and prognostic markers are not yet available to assess iron overload-induced liver fibrogenesis and progression in HCV infections. Here, by means of Spike-in SILAC proteomic approach, we first unveiled a specific membrane protein expression signature of HCV cell cultures in the presence of iron overload. Computational analysis of proteomic dataset highlighted the hepatocytic vitronectin expression as the most promising specific biomarker for iron-associated fibrogenesis in HCV infections. Next, the robustness of our in vitro findings was challenged in human liver biopsies by immunohistochemistry and yielded two major results: (i) hepatocytic vitronectin expression is associated to liver fibrogenesis in HCV-infected patients with iron overload; (ii) hepatic vitronectin expression was found to discriminate also the transition between mild to moderate fibrosis in HCV-infected patients without iron overload.

Received: September 26, 2013
Revised: January 8, 2014
Accepted: January 9, 2014

Keywords:
Biomedicine / Hepatitis C infection / Liver fibrosis / Hepatic iron overload / Vitronectin

Additional supporting information may be found in the online version of this article at the publisher's web-site

1 Introduction

Liver fibrosis, the common outcome of chronic inflammatory diseases, is the result of the wound-healing response of the organ to repeated injury; this process causes distortion of the hepatic architecture by forming a fibrous scar and nodules

Correspondence: Professor Marco Tripodi, Department of Cellular Biotechnologies and Haematology, Istituto Pasteur-Fondazione Cenci Bolognetti, Sapienza University of Rome, Via Regina Elena 324, 00161 Rome, Italy
E-mail: tripodi@bce.uniroma1.it
Fax: +39-06-0644252865

Abbreviations: **HCC**, hepatocellular carcinoma; **HCV**, hepatitis C virus; **HCVcc**, cell culture-derived HCV; **HSC**, hepatic stellate cell

*Current address: Dr. Simone Mattei, European Molecular Biology Laboratory, Meyerhofstrasse 1, Heidelberg 69117, Germany

Our findings provide first observational evidences on the molecular effects of viral-induced iron overload and allow for hypothesizing on new diagnostic tools.

Colour Online: See the article online to view Figs. 1, 2 and 4 in colour.

of regenerating hepatocytes (liver cirrhosis), thus leading to liver failure and eventually hepatocellular carcinoma (HCC) [1]. Early diagnosis of fibrosis is crucial, and developing reliable diagnostic markers for its onset and progression is an important goal in clinical hepatology.

Hepatitis C virus (HCV), estimated to chronically infect more than 170 million individuals worldwide, is one of main causes of liver fibrosis [2]. Commonly, in HCV-infected patients, liver fibrosis located in the portal tracts develops late and remains stable over a long time [3]. However, in many cases its onset and progression to cirrhosis is influenced by comorbidity factors that include alcohol consumption, metabolic syndromes, coinfections with human immunodeficiency virus, and hepatic iron overload [3, 4].

HCV-associated pathological iron deposits, ascribed to the viral-induced inhibition of the iron regulatory hormone hepcidin, are observed in approximately 40% of chronic infections [5, 6]. Long-lasting iron overload exerts a negative influence on liver fibrosis [7–9]; it also been observed that iron depletion therapy reduces the risk of developing severe fibrosis in HCV patients [10]. Iron-induced liver fibrosis is principally attributable to oxidative damages [11]. In fact, the increased production of ROS is responsible for several molecular changes leading to the perturbation of normal cellular morphology [12, 13]. In the viral-independent (e.g. genetic) iron overload diseases, the iron deposits affect the entire parenchyma and oxidative damage affects most of the hepatocytes [14]. On the contrary, in HCV infections iron deposits are observed almost exclusively in the periportal areas and colocalize with the initial fibrous scars [15]. This limited distribution has hampered in vivo molecular investigations of the interaction between intracellular viral infection and iron excess. Here, at aiming to identify potential early markers for the iron-induced liver fibrosis in HCV infections, we circumvent this hindrance by firstly performing a "Spike-in" stable-isotope labeling with amino acids in cell culture (Spike-in SILAC) proteomic approach on HCV-infected cells in presence of iron overload. A significant subset of specifically modulated proteins was identified. A computational analysis of proteomic datasets highlighted that the interaction between viral infection and iron excess strongly upregulates vitronectin expression. Our investigations on vitronectin expression were then extended to in vivo samples. In particular, studies on human liver biopsies highlighted that hepatocytic vitronectin production is an early molecular signature of viral-associated liver fibrosis in presence of iron overload and discriminates the transition between mild to moderate fibrosis in HCV-infected patients.

2 Materials and methods

2.1 Ethics statement

The study has been approved by the ethics committee of the INMI "L. Spallanzani" IRCCS, Rome, Italy, according to the ethical guidelines of the 1975 Declaration of Helsinki. Analyses on human liver biopsies and sera were carried out on clinical samples and analyzed anonymously. To protect patient confidentiality, all patient identifiers were removed from the samples to make them completely anonymous.

2.2 Reagents

The chemicals, reagents, and suppliers that were used are listed below: TEMED, SDS, Tween 20, BSA, PBS, DMEM, trypsin-EDTA solution, FBS, L-glutamine, penicillin/streptomycin, trifluoroacetic acid, Ponceau S solution, α-cyano-4-hydroxycinnamic acid, paraformaldehyde, Triton X-100, sodium chloride, EDTA, protease inhibitor cocktail, DTT, iodoacetamide, N-acetyl cysteine, and ammonium bicarbonate were purchased from Sigma-Aldrich (St. Louis, MO). Bradford Bio-Rad Protein Assay, Page Ruler tm Plus Prestained Protein Ladder Fermentas Life Sciences (Vilnius, Lithuania). NuPAGE gel electrophoresis reagents Simply Blue Safe Stain were obtained from Invitrogen (Carlsbad, CA). SILAC media DMEM was purchased from Silantes (Munich, Germany). Nytrocellulose membranes (Protran BA85) were obtained from Whatman-Schleicher & Schuel (Dassel, Germany). ECL Plus Western Blotting Detection System was purchased from GE Healthcare (Chalfont St. Giles, UK). Methanol and ACN were purchased from J.T. Baker (Phillipsburg, NJ) and Microcolumn ZipTip (μ-C18) were purchased from Millipore Corporation (Ballerica, MA). Anti Vitronectin antibody was purchased from Santa Cruz (Dallas, TX). Anti-GAPDH antibody and Membrane Protein Extraction Kit (M-PEK) were purchased from Calbiochem Merck (Gibbstown, NJ).

2.3 In vitro production of the HCV infectious particles and cell culture

The clone used for HCV particles production was the designated JFH-1, derived from a Japanese patient with fulminant hepatitis, kindly provided by Dr. T. Wakita [16, 17]. The highly permissive Huh7.5-derived cell line designated Huh7.5.1 used for viral particles production was kindly provided by Prof. F. Chisari [18].

All cells were maintained in a monolayer at 37°C in 5% CO_2. For cell culture-derived HCV (HCVcc) production, Huh7.5.1 cells were infected with JFH-1-derived virus (genotype 2a) (MOI = 0.1). In order to induce iron overload, after 5 day of cultivation, Huh7.5.1 cells were treated with iron excess by means of $FeSO_4$/8-Hydroxyquinoline 10 μM for 30 min that has been shown to be nontoxic to cells [19]. After 6 days of cultivation, cells were lysed and membrane proteins were isolated following the Membrane Protein Extraction Kit (M-PEK) protocol. Samples were analyzed by Bradford assay to determine the protein concentration, then dissolved in SDS-loading buffer and analyzed by Western blotting.

2.4 SILAC labeling of human-cultured hepatocytes

Huh7 5.1 cells and Huh7 5.1 treated cells (i.e.: iron overload, HCV infection, or both conditions) were respectively grown in SILAC "heavy" ($^{13}C_6$ $^{15}N_4$-arginine and $^{13}C_6$-lysine) and SILAC "light" ($^{12}C_6$ $^{14}N_4$-arginine and $^{12}C_6$-lysine) conditions for eight passages before the experiment. This period lasted about 3 weeks, where the SILAC "heavy" cells' labeling was complete.

Equal amounts (150 μg) of membrane proteins from Huh7.5.1 and Huh7.5.1 treated with iron overload, HCV infection or both the conditions were mixed and analyzed by SDS-PAGE and nanoLC-MALDI. At least three independent biological and technical replicates were performed.

2.5 Protein digestion, peptide purification, nanoLC analysis, MS analysis

Hundred micrograms of membrane proteins obtained from the SILAC experiment were separated on 4−12% gradient gels (Invitrogen), stained by Simply Blue Safe Stain staining and visualized. Sixteen sections of the gel lane were cut. Protein digestion of gel pieces, peptide purification, and LC-MS/MS analysis were performed as previously described [20].

2.6 Data analysis

Matrix2png program (http://www.chibi.ubc.ca/matrix2png/) was used for making heat-map visualizations of protein data expression. Proteins were ordered through a hierarchical Euclidean clustering algorithm using the Babelomics 4.2 (http://babelomics.bioinfo.cipf.es) [21]. Gene ontology analysis was performed by a functional profiling tool in Babelomics 4.2. Right-tailed Fisher's exact test was used to calculate a *p*-value determining the probability that each biological function and/or disease involved in that proteome profile alteration is due to chance alone. To identify the biomarkers that are unique for the HCV + Fe cells, proteomic dataset for each experimental condition were also analyzed by the IPA biomarker comparison function.

2.7 Western blotting assay

Western blotting analyses were performed as described in Mancone et al. [20].

2.8 Immunostaining

Immunohistochemical procedures were performed on formalin-fixed paraffin-embedded tissue sections (4 μm) according to Carpenter et al. [22]. Santa Cruz Biotechnology polyclonal rabbit Vitronectin 65/75 (H-270) was used as primary antibody (appropriately diluted 1:200). The sections were evaluated by light microscopic examination and cellular localization and intensity of immunostaining in each section were assessed by two pathologist observers (A.B.; F.D.N.). Individual cases were considered IR for individual antigens when more than 5% of the cells were IR. IR cases were further classified as follows: + = 5–10% IR cells; ++ = 11–50% IR cells; +++ = >50% IR cells. Given the strong and consistent expression of vitronectin immunoreactivity in the advanced fibrotic liver hepatocytes, we also evaluated the staining intensity of vitronectin as faint (+), moderate (++), and strong (+++) in respect to non-IR hepatocytes. Histological assessment of iron overload was performed by Perls' Prussian blue assay and the hepatocytic iron content (hepatocytic iron score) was evaluated according to Deugnier's grading [23].

2.9 Immunofluorescent microscopy

For immunofluorescence analysis, cells were fixed with 4% paraformaldehyde, permeabilized with 0.2% Triton, blocked with 10% donkey serum and then incubated with an anti-CORE antibody (Anogen) and anti-Bip (Santa Cruz sc1051) for 1 h. After being washed, cells were incubated with CyTM2-conjugated AffiniPure F(ab')$_2$ fragment donkey anti-mouse IgG (ImmunoResearch Laboratories, INC.) and Alexa Fluor 488 donkey anti-goat IgG (Invitrogen) secondary antibodies for 30 min.

2.10 Real-time PCR

Cellular RNA was prepared with Trizol reagent (Invitrogen), cDNA synthesis was generated from 1 μg of RNA using the reverse transcription kit (Promega) according to manufacturer's recommendations. Real-time PCR reactions were performed with the LightCycler (Roche) using the LightCycler FastStart DNA Master SYBR-Green-I (Roche) according to the manufacturer's instructions. Five microliters of 1:10 cDNA dilution cDNA was used as template and cycling parameters were 95°C for 10 min, followed by 40 cycles of 95°C for 10 s, 62°C for 10 s, 72°C for 10 s. Relative amounts were obtained using the $2^{-\Delta\Delta Ct}$ method normalized for the L34 gene expression. Primer sets for all amplicons were:

HCVcc forward: 5′-TCTGCGGAACCGGTGAGTA-3′
HCVcc reverse: 5′-TCAGGCAGTACCACAAGGC-3′
L34 forward: 5′-GTCCCGAACCCCTGGTAATAG-3′
L34 reverse: 5′-GGCCCTGCTGACATGTTTCTT-3′

3 Results

3.1 Iron overload drastically perturbs the membrane proteome profiles of cultured hepatoma cells

Morphological alterations of cell architecture in response to injuries involve changes in cell surface protein expression and in the specific release of secreted proteins. Therefore, both

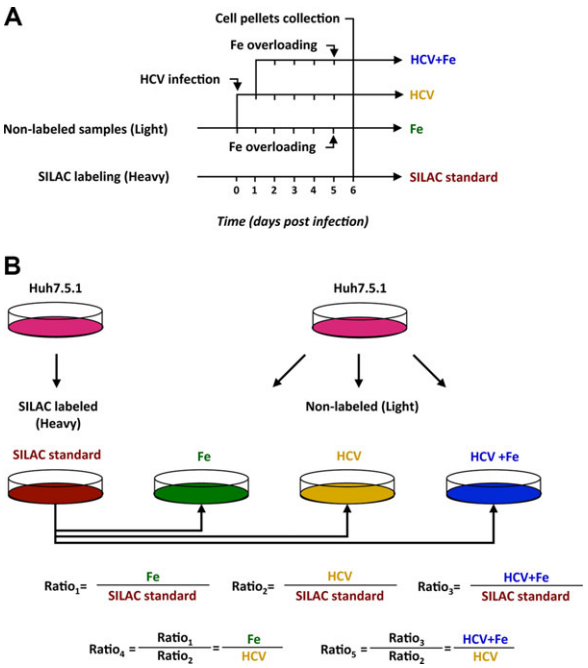

Figure 1. Spike in SILAC workflow. (A) Spike-in SILAC standard labeling (Huh7.5.1 Heavy) was "decoupled" from the biological experiments and then carried out under normal cell culture conditions (Huh7.5.1 Light). Each treatment was performed and subsequently analyzed in triplicate. (B) After the treatments were performed, the nonlabeled samples were combined with the SILAC standard and each of these combined samples was analyzed separately by LC-MS/MS. Ratio 1 originated from the light/heavy ratio between iron-overloaded cells (Fe) and SILAC standard; Ratio 2 from HCV-infected cells (HCV) and SILAC standard; Ratio 3 from iron-overloaded and HCV-infected cells (HCV + Fe) and SILAC standard. Differences between the experimental samples were calculated as the 'ratio of ratios', where the ratio of one sample relative to the standard is divided by the ratio of the other relative to the standard (Ratios 4 and 5).

the plasma membrane and the intracellular secretory vesicles represent a rich source for discovering novel biomarkers in fibrogenesis.

In order to identify possible biomarkers of iron-induced liver fibrosis in HCV infections, we performed a quantitative proteomic analysis on highly native membrane purifications of HCV-infected cells (JFH-1 HCVcc) treated with an excess of iron. In particular, we applied the Spike-in SILAC strategy that allows for multiple quantitative comparisons among samples by means of a unique internal standard (SILAC standard) [24]. To this end, we metabolically labeled Huh7–5.1 cells with $^{13}C_6$ $^{15}N_4$-arginine and $^{13}C_6$-lysine (Heavy) for SILAC standard production. Nonlabeled cell populations were instead grown in light medium ($^{12}C_6$ $^{14}N_4$-arginine and $^{12}C_6$-lysine) and subsequently subject to HCV-infection with and without iron overload (Fig. 1A). Notably, a previous study performed on a similar cell line (Huh7.5) and HCV strain (J6/JFH1) demonstrated that HCV infection at 1 and 3 days postinfection profoundly perturbs the global proteome profile [25]. We here therefore performed our investigations at 6 days postinfection; this to avoid acute phase-induced alterations in proteins expression and to obtain a higher frequency of infected hepatocytes (Supporting Information 1). Moreover, since previous reports performed with subgenomic HCV replicon [26] and with HCV-infected Huh7–5.1 cells (JFH-1 HCVcc) [27] systems indicated that iron overload affects the expression of viral RNA and proteins, we also investigated on HCV replication and infection. In line with the published results, we found that iron excess downregulates intracellular viral RNA and core protein antigen (Supporting Information 2).

Therefore, for proteomics analysis, cell extracts were isolated separately and each nonlabeled sample was combined with equal amounts of SILAC standard cell extract (Fig. 1B). Finally, pooled samples were then enriched in plasma membrane and the intracellular secretory vesicles (Supporting Information 3) and isolated proteins were subsequently subjected to nanoLC-MALDI-TOF/TOF analysis.

Among 803 detected proteins, 74, exhibiting abundance changes ≥1.5-fold increase (Supporting Information 4) were analyzed by means of a hierarchical clustering algorithm that allowed for grouping similar samples based on the pattern of fold-change in protein abundance (Babelomics 4.2). Then, by using heat maps (Matrix2png, version 1.2.2), the protein expression levels of HCV-infected cells with iron overload (HCV + Fe, $Ratio_3$) were compared with those of the two conditions separately (Fe, $Ratio_1$; HCV, $Ratio_2$) (Fig. 2A).

Interestingly, while HCV at 6 days after infection only partially modified protein expression, cells treated with iron underwent dramatic changes in their membrane proteome profiles. Since we were interested in proteins specifically modulated when the HCV infection occurs in a context of iron overload, we focused our attention on the protein pattern in the HCV + Fe condition. To this end, we calculated the ratios Fe/HCV ($Ratio_4$) and (HCV + Fe)/HCV ($Ratio_5$) (Fig. 1B and Supporting Information 4). Interestingly, as shown in Fig. 2B, the HCV + Fe profile shows a few but significant differences in respect to the Fe profile (Fig. 2B). The gene ontology analysis revealed that the copresence of iron and HCV causes impairment of the membrane proteome profile in a broad range of biological processes, including cell–cell adhesion, cell–extracellular matrix interactions, cell migration, cell proliferation, and survival (Supporting Information 5).

3.2 Iron overload in HCV-infected cells causes upregulation of vitronectin expression

To identify potential biomarkers specific for the comorbidity between HCV and iron overload, the proteomic datasets were then analyzed by the biomarker module of the IPA analysis program. This application has led to ranking and prioritization of the identified potential marker genes in HCV + Fe cells. The membrane-associated vitronectin, a multifunctional plasma and extracellular matrix protein produced

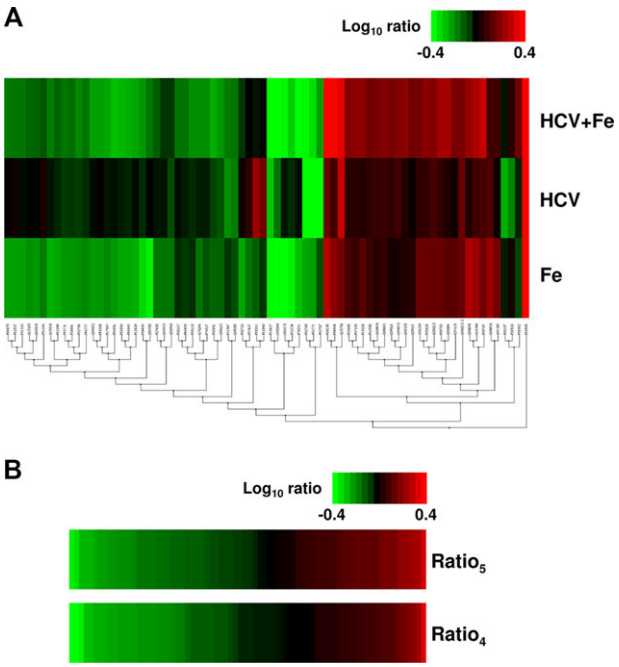

Figure 2. Iron overload perturbs the proteome profile of the HCV-infected cells. (A) Two-dimensional hierarchical clustering analysis with a weighted Euclidean method of differentially regulated proteins (Babelomics 4.2). Each horizontal row represents an individual condition and each vertical column an individual protein. Protein abundance ratios were colored according to the fold changes (green Log_{10} ratios: downregulations; red Log_{10} ratios: upregulations) and the color scale indicates the magnitude of expression changes. Black squares indicate no change in protein abundance. The clustering tree is shown. (B) Heat map analysis of $Ratio_4$ and $Ratio_5$. Each vertical column represents an individual protein. Protein abundance ratios were colored according to the fold changes (green Log_{10} ratios: downregulations; red Log_{10} ratios: upregulations) and the color scale indicates the magnitude of expression changes. Black squares indicate no change in protein abundance.

by hepatocytes, resulted as the top rank product (Table 1 and Supporting Information 6). This result was confirmed and further extended by analyzing both membranes and whole cell extract by Western blotting. As shown in Fig. 3,

Table 1. IPA biomarker comparison: top five proteins in common biomarkers list

Gene name	Protein name	Fe[a)]	HCV[a)]	HCV + Fe[a)]
VTN	Vitronectin	1.63	1.30	2.77
SLC3A2	4F2 cell-surface antigen heavy chain (CD98)	1.92	1.48	2.64
SLC1A5	Solute carrier family 1	1.50	2.10	2.24
KRT8	Cytokeratin-8	1.51	1.30	2.05
GNA13	Guanine nucleotide binding protein	1.73	1.83	1.83

a) Fold change in respect to Silac standard.

vitronectin expression was found induced in HCV-infected cells with iron overload, thus confirming proteomic results.

Since several reports characterized vitronectin as a reliable immunomarker of mature liver fibrosis and hepatocellular carcinoma [28–31], we decided to challenge the robustness of this observation in HCV-infected patients.

3.3 Hepatocytic vitronectin production is an early marker of iron associated-liver fibrosis in HCV-infected patients

Forty paraffin-embedded formalin-fixed liver samples at different stages of liver fibrosis (F1–F4 according to Metavir score) were collected from male treatment naïve patients infected with HCV genotype 1 (Table 2). HCV-related hepatic iron accumulation has been shown to be present mainly in male patients [5], and HCV genotype 1 has been shown to be responsible for most of the chronic infections in Western countries.

Samples were then assayed for HCV-related hepatocytic iron overload and the vitronectin expression levels were then evaluated by IHC analysis (Table 2). The results showed particular significance at the early stages of the fibrotic process: while the vitronectin staining distribution was limited to the portal tract connective tissue (Fig. 4A) in most of the non-iron overload patients (HCV), all of the patients with increased iron accumulation (HCV + Fe) showed intracellular vitronectin immunostaining. In particular, the staining intensity was found to be moderate or strong in the periportal hepatocytes and faint in the pericentral area (Table 2 and Fig. 4A). Notably, staining for iron deposits highlighted the same peculiar distribution. Overall, as shown in Fig. 4B, hepatocytic vitronectin distribution colocalized with the pathological iron deposits of the periportal area, and the hepatocytic iron score was found to correlate with vitronectin staining intensity ($r = 0.79$, $p < 0.00003$).

In advanced fibrosis (F3–F4), independent from iron accumulation, both the hepatocytic and extracellular immunoreactivities were found increased in respect to those observed in the early fibrotic stages (Table 2 and Fig. 4A). These data indicate that the hepatic vitronectin expression also discriminates the transition between mild to moderate fibrosis in patients without iron overload. Conversely, no significant alterations in vitronectin plasma concentration were detected (data not shown), maybe due to the high concentration levels of circulating protein.

Altogether, these results indicate that hepatocytic vitronectin expression shows a potential diagnostic yield in the assessment of iron overload-associated liver fibrogenesis and in discriminating disease progression (Fig. 4C).

4 Discussion

Currently, neither diagnostic nor prognostic tools are available to assess the effects of HCV-related hepatic iron

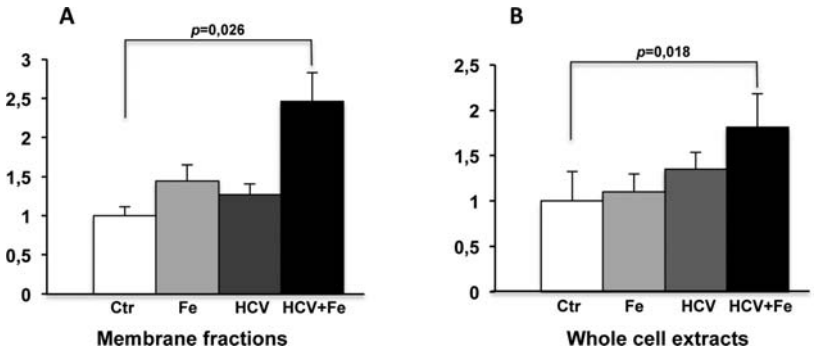

Figure 3. Vitronectin is upregulated in HCV-infected cells with iron overload. Proteins from membrane fractions and whole cell extracts were separated by SDS-PAGE and transferred to a PVDF membrane. Vitronectin, GAPDH, and calnexin were detected with respective antibodies. Bands were analyzed by densitometry using Quality-One software (Bio-Rad laboratories, Richmond, CA). The X axis shows the relative intensity of vitronectin/calnexin (A) and vitronectin/GAPDH (B) in the indicated conditions. All data were from at least three independent experiments and shown as mean ± SD.

Table 2. Clinicopathological features and vitronectin immunohistochemical results of the series

Liver fibrosis Metavir score	Patient	Age	Activity grade	Hepatocytic iron score	Vitronectin immunoreactivity	Vitronectin staining intensity
F1	1	54	3	0	/	/
	2	33	3	0	/	/
	3	41	3	0	/	/
	4	52	3	0	+	+
	5	30	3	0	/	/
F1	6	57	3	9	+	+
	7	31	3	3	++	++
	8	36	3	9	+++	+++
	9	38	3	9	+++	++
	10	49	3	12	++	++
F2	11	52	3	0	+	+
	12	51	3	0	/	/
	13	48	3	0	/	/
	14	53	3	0	/	/
	15	44	3	0	+	+
F2	16	55	3	6	+	+
	17	55	3	6	+	+
	18	51	3	18	+++	+++
	19	43	3	6	++	+
	20	53	3	15	++	++
F3	21	33	3	0	+++	++
	22	61	3	0	+++	++
	23	47	3	0	++	++
	24	49	3	0	++	++
	25	47	3	0	++	+
F3	26	51	3	6	+++	+++
	27	48	3	3	++	++
	28	61	3	18	+++	+++
	29	50	3	6	++	++
	30	52	3	6	++	++
F4	31	50	3	0	+++	++
	32	42	3	0	+++	++
	33	51	3	0	+++	+++
	34	69	3	0	+++	+++
	35	49	3	0	+++	+++
F4	36	55	3	9	+++	+++
	37	55	3	3	+++	+++
	38	53	3	3	+++	+++
	39	51	3	3	++	++
	40	50	3	9	+++	+++

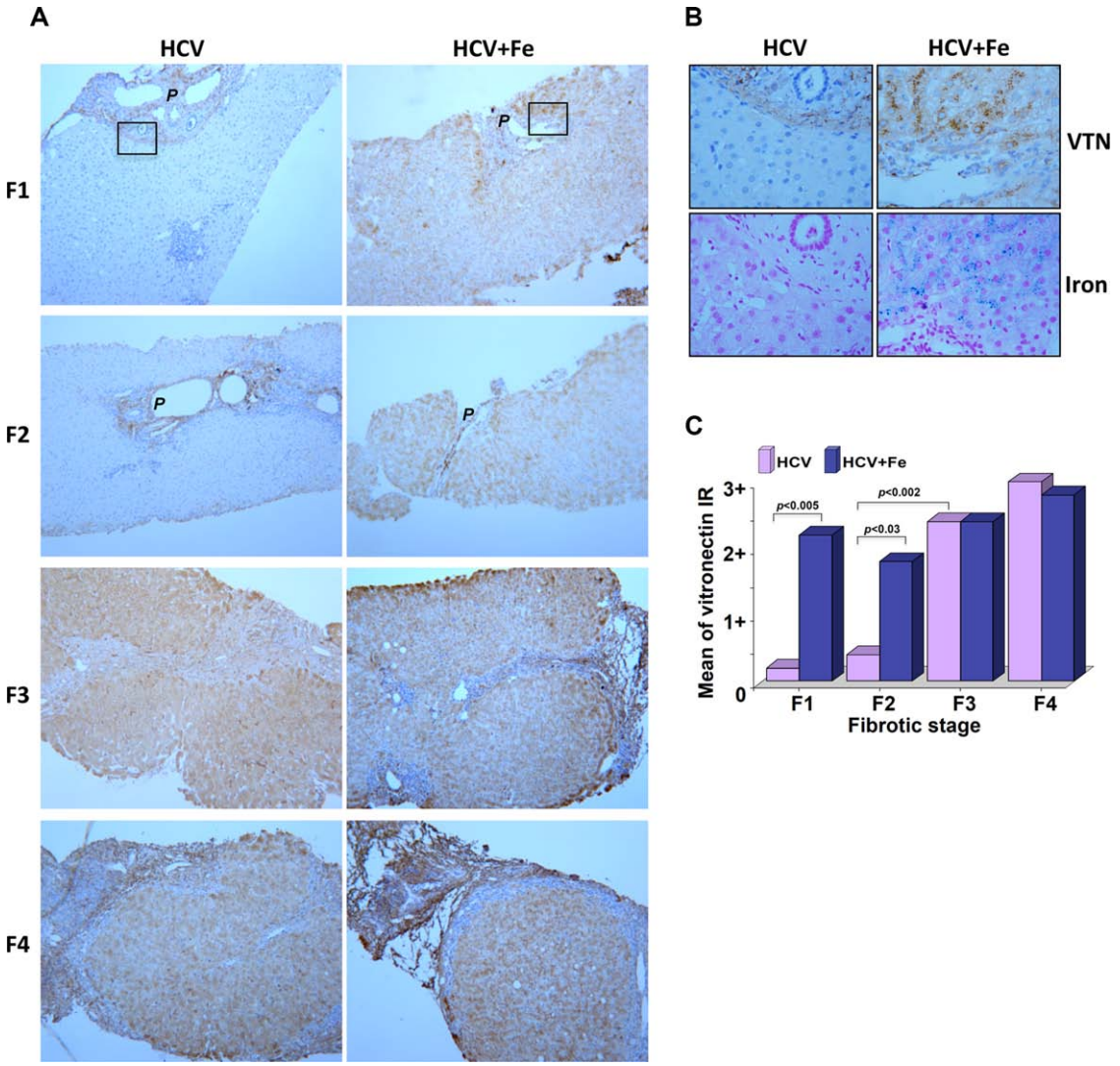

Figure 4. HCV-infected patients with hepatic iron overload already show hepatocytic vitronectin immunoreactivity in minimal and mild fibrosis. (A) Vitronectin immunostaining on hepatic FFPE of HCV-infected patients with (HCV + Fe) and without (HCV) iron accumulation at different stages of liver fibrosis (F1–F4). Portal tracts are indicated (*P*); squares indicate magnifications showed in B. (Original magnifications ×10). (B) Vitronectin immunostaining and Perls' Prussian blue assay on hepatic FFPE with (HCV + Fe) and without (HCV) iron accumulation in the fibrotic stage F1. (Original magnifications ×40). (C) Histogram summarizing the mean values of vitronectin immunoreactivities (see Table 2) of HCV-infected patients with (HCV + Fe) and without (HCV) hepatocytic iron accumulation.

accumulation on liver fibrosis onset and progression. Here, combining in vitro and in vivo approaches, we identified the vitronectin as a promising early marker of liver fibrosis in the HCV infections with hepatic overload.

HCV-induced iron overload only regards a small number of hepatocytes located in the periportal tract, thus limiting a large-scale molecular investigation of in vivo samples. The in vitro cellular model has been instrumental to this investigation. The introduction of the JFH-1 HCVcc natural infection system has led to important advances in the study of relationship between HCV and the host metabolism [17]; this in vitro model allowed for recapitulating a microenvironment where the complete viral life cycle occurred in a context of iron excess. The proteomic strategy Spike-in SILAC led us to unveil a specific protein expression signature of HuH7.5.1 cells in the presence of HCV, iron, and HCV and iron. In fact, as Mann and coworkers showed, this extension of the SILAC approach allows quantitative comparisons of several different biological samples. A computational analysis on proteomic datasets highlighted vitronectin as the most promising specific biomarker for iron-induced fibrogenesis. The correlation between hepatocytic vitronectin overexpression and HCV-induced hepatic iron overload was then challenged in human liver biopsies. This analysis highlighted two major evidences; (i) hepatocytic vitronectin expression is associated to liver fibrogenesis in HCV-infected patients with iron

overload, (ii) hepatic vitronectin expression was found to discriminate the transition between F2 and F3 fibrotic stages also in patients without iron overload.

Vitronectin is a multifunctional glycoprotein produced by hepatocytes, encapsulated in secretory vesicles, and released in the extracellular space principally as serum protein and, in the liver and in a variety of tissues, as component of the extracellular matrix [32, 33]. This protein provides a unique regulatory link among cell adhesion, differentiation, proliferation, and morphogenesis: (i) it promotes cell proliferation, spreading, and migration by interaction between specific integrins, (ii) it is involved in the immune defense through interaction with the complement system, and (iii) it is implicated in the formation and dissolution of blood clots [34].

Activated hepatic stellate cells (HSCs) have been identified as major collagen-producing cells in injured liver, thus playing play a central role in the development of liver fibrosis [1]. In liver fibrogenesis, upregulation of αvβ3 integrin, a specific vitronectin receptor, contributes to the activation and proliferation of HSC [35–37]. In addition, vitronectin is involved in recruiting and positioning lymphocytes within inflamed and malignant liver tissue, thus leading to HSC activation [38]. In light of these evidences, it is conceivable that increased hepatic vitronectin expression favors also the fibrogenesis.

Vitronectin is found at low concentrations in normal extracellular matrix and increased in chronic inflammatory liver disease, where its deposition in ECM is indicative of mature fibrosis [28–30]. Our results extend the potential diagnostic yield of vitronectin in HCV-related liver fibrosis in presence of iron overload. In fact, we highlighted an intracellular vitronectin upregulation as early as in liver fibrosis stage F1. Moreover, since in vitro and in vivo data were obtained with different HCV genotype (i.e.: genotype 2 for JFH-1-derived virus and genotype 1 for infected donors) it seems conceivable that vitronectin upregulation is a general feature of HCV infection.

In the last years several reports demonstrated that the HCV-induced iron overload exerts a negative influence on liver disease. In fact, iron accumulation induces liver steatosis (by increasing lipidogenesis and reducing intracellular lipid catabolism and apoB-100-containing lipoprotein secretion) and HCC [20, 39, 40]. Moreover, HCV-infected patients with hepatic iron overload are at high risk of liver fibrosis: hepatic iron excess has been positively correlated to fibrosis progression ($r = 0.356$; $p = 0.0003$), to inflammatory activity ($r = 0.248$; $p = 0.00121$), to aspartate transaminase ($r = 0.247$; $p = 0.0126$), and indirectly to platelet count ($r = -0.369$; $p = 0.0002$) [9]. In light of these observations, we believe that monitoring and counteracting hepatic iron levels, so far only considered within the framework of interferon-based therapy [41], may be a valid antifibrotic strategy. In this context, the assessment of hepatic vitronectin expression and its zonal distribution could represent the read-out of the pathological iron effects even at first stage of hepatic fibrosis; future clinical investigations may challenge the robustness of these insights.

In conclusion, we identified hepatocytic vitronectin as the first iron-associated specific signature of liver fibrogenesis in HCV infections. Our findings have implications for better understanding the effects of iron as a comorbid factor of chronic hepatitis C and suggest a potential clinical impact of iron depletion therapy to counteract disease progression.

We are grateful to Enrico Girardi and Paola Scognamiglio for their helpful comments. We are deeply grateful to Ms. Andrea Baker (INMI Rome, Italy) for the editing, to Dr. Takaji Wakita for providing HCVcc and to Prof Frank C. Chisari for providing Huh7.5.1 cells.

This work was supported by grants from MIUR Ministero dell'Università e Ricerca Scientifica (FIRB 2012, codice progetto RBFR12NSCF), Associazione Italiana per la Ricerca sul Cancro (AIRC) and Ministero della Salute (Ricerca Finalizzata 40H27, Ricerca Corrente).

The authors have declared no conflict of interest.

5 References

[1] Bataller, R., Brenner, D. A., Liver fibrosis. *J. Clin. Invest.* 2005, *115*, 209–218.

[2] Ly, K. N., Xing, J., Klevens, R. M., Jiles, R. B. et al., The increasing burden of mortality from viral hepatitis in the United States between 1999 and 2007. *Ann. Intern. Med.* 2012, *156*, 271–278.

[3] Marcellin, P., Asselah, T., Boyer, N., Fibrosis and disease progression in hepatitis C. *Hepatology* 2002, *36*, S47–S56.

[4] Feld, J. J., Liang, T. J., Hepatitis C–identifying patients with progressive liver injury. *Hepatology* 2006, *43*, S194–S206.

[5] Farinati, F., Cardin, R., De Maria, N., Della Libera, G. et al., Iron storage, lipid peroxidation and glutathione turnover in chronic anti-HCV positive hepatitis. *J. Hepatol.* 1995, *22*, 449–456.

[6] Nishina, S., Hino, K., Korenaga, M., Vecchi, C. et al., Hepatitis C virus-induced reactive oxygen species raise hepatic iron level in mice by reducing hepcidin transcription. *Gastroenterology* 2008, *134*, 226–238.

[7] Corengia, C., Galimberti, S., Bovo, G., Vergani, A. et al., Iron accumulation in chronic hepatitis C: relation of hepatic iron distribution, HFE genotype, and disease course. *Am. J. Clin. Pathol.* 2005, *124*, 846–853.

[8] Tung, B. Y., Emond, M. J., Bronner, M. P., Raaka, S. D. et al., Hepatitis C, iron status, and disease severity: relationship with HFE mutations. *Gastroenterology* 2003, *124*, 318–326.

[9] Fujita, N., Sugimoto, R., Urawa, N., Araki, J. et al., Hepatic iron accumulation is associated with disease progression and resistance to interferon/ribavirin combination therapy in chronic hepatitis C. *J. Gastroenterol. Hepatol.* 2007, *22*, 1886–1893.

[10] Angelucci, E., Muretto, P., Nicolucci, A., Baronciani, D. et al., Effects of iron overload and hepatitis C virus positivity in

determining progression of liver fibrosis in thalassemia following bone marrow transplantation. *Blood* 2002, *100*, 17–21.

[11] Sumida, Y., Yoshikawa, T., Okanoue, T., Role of hepatic iron in non-alcoholic steatohepatitis. *Hepatol. Res.* 2009, *39*, 213–222.

[12] Dongiovanni, P., Fracanzani, A. L., Fargion, S., Valenti, L., Iron in fatty liver and in the metabolic syndrome: a promising therapeutic target. *J. Hepatol.* 2011, *55*, 920–932.

[13] Lee, K. S., Buck, M., Houglum, K., Chojkier, M., Activation of hepatic stellate cells by TGF alpha and collagen type I is mediated by oxidative stress through cmyb expression. *J. Clin. Invest.* 1995, *96*, 2461–2468.

[14] Deugnier, Y., Turlin, B., Pathology of hepatic iron overload. *Semin. Liver. Dis.* 2011, *31*, 260–271.

[15] Isom, H. C., McDevitt, E. I., Moon, M. S., Elevated hepatic iron: a confounding factor in chronic hepatitis C. *Biochim. Biophys. Acta* 2009, *1790*, 650–662.

[16] Kato, T., Furusaka, A., Miyamoto, M., Date, T. et al., Sequence analysis of hepatitis C virus isolated from a fulminant hepatitis patient. *J. Med. Virol.* 2001, *64*, 334–339.

[17] Wakita, T., Pietschmann, T., Kato, T., Date, T. et al., Production of infectious hepatitis C virus in tissue culture from a cloned viral genome. *Nat. Med.* 2005, *11*, 791–796.

[18] Zhong, J., Gastaminza, P., Cheng, G., Kapadia, S. et al., Robust hepatitis C virus infection in vitro. *Proc. Natl. Acad. Sci. USA* 2005, *102*, 9294–9299.

[19] Van Lenten, B. J., Prieve, J., Navab, M., Hama, S. et al., Lipid-induced changes in intracellular iron homeostasis in vitro and in vivo. *J. Clin. Invest.* 1995, *95*, 2104–2110.

[20] Mancone, C., Montaldo, C., Santangelo, L., Di Giacomo, C., Ferritin heavy chain is the host factor responsible for HCV-induced inhibition of apoB-100 production and is required for efficient viral infection. *J. Proteome Res.* 2012, *11*, 2786–2797.

[21] Medina, I., Carbonell, J., Pulido, L., Madeira, S. C. et al., Babelomics: an integrative platform for the analysis of transcriptomics, proteomics and genomic data with advanced functional profiling. *Nucleic Acids Res.* 2010, *38*, W210–W213.

[22] Carpenter, B., McKay, M., Dundas, S. R., Lawrie, L. C. et al., Heterogeneous nuclear ribonucleoprotein K is over expressed, aberrantly localised and is associated with poor prognosis in colorectal cancer. *Br. J. Cancer* 2006, *95*, 921–927.

[23] Deugnier, Y. M., Loréal, O., Turlin, B., Guyader, D. et al., Liver pathology in genetic hemochromatosis: a review of 135 homozygous cases and their bioclinical correlations. *Gastroenterology* 1992, *102*, 2050–2059.

[24] Geiger, T., Wisniewski, J. R., Cox, J., Zanivan, S. et al., Use of stable isotope labeling by amino acids in cell culture as a spike-in standard in quantitative proteomics. *Nat. Protoc.* 2011, *6*, 147–157.

[25] Diamond, D. L., Syder, A. J., Jacobs, J. M., Sorensen, C. M. et al., Temporal proteome and lipidome profiles reveal hepatitis C virus-associated reprogramming of hepatocellular metabolism and bioenergetics. *PLoS Pathog.* 2010, *6*, e1000719.

[26] Fillebeen, C., Rivas-Estilla, A. M., Bisaillon, M., Ponka, P. et al., Iron inactivates the RNA polymerase NS5B and suppresses subgenomic replication of hepatitis C Virus. *J. Biol. Chem.* 2005, *280*, 9049–9057.

[27] Fillebeen, C., Pantopoulos, K., Iron inhibits replication of infectious hepatitis C virus in permissive Huh7.5.1 cells. *J. Hepatol.* 2010, *53*, 995–999.

[28] Koukoulis, G. K., Shen, J., Virtanen, I., Gould, V. E., Vitronectin in the cirrhotic liver: an immunomarker of mature fibrosis. *Hum. Pathol.* 2001, *32*, 1356–1362.

[29] Kobayashi, J., Yamada, S., Kawasaki, H., Distribution of vitronectin in plasma and liver tissue: relationship to chronic liver disease. *Hepatology* 1994, *20*, 1412–1417.

[30] Inuzuka, S., Ueno, T., Torimura, T., Tamaki, S. et al., Vitronectin in liver disorders: biochemical and immunohistochemical studies. *Hepatology* 1992, *15*, 629–636.

[31] Paradis, V., Degos, F., Dargère, D., Pham, N. et al., Identification of a new marker of hepatocellular carcinoma by serum protein profiling of patients with chronic liver diseases. *Hepatology* 2005, *41*, 40–47.

[32] Hayman, E. G., Pierschbacher, M. D., Ohgren, Y., Ruoslahti, E., Serum spreading factor (vitronectin) is present at the cell surface and in tissues. *Proc. Natl. Acad. Sci. USA* 1983, *80*, 4003–4007.

[33] Seiffert, D., Constitutive and regulated expression of vitronectin. *Histol. Histopathol.* 1997, *12*, 787–797.

[34] Schvartz, I., Seger, D., Shaltiel, S., Vitronectin. *Int. J. Biochem. Cell Biol.* 1999, *31*, 539–544.

[35] Zhou, X., Murphy, F. R., Gehdu, N., Zhang, J. et al., Engagement of alphavbeta3 integrin regulates proliferation and apoptosis of hepatic stellate cells. *J. Biol. Chem.* 2004, *279*, 23996–24006.

[36] Patsenker, E., Popov, Y., Wiesner, M., Goodman, S. L., Schuppan, D., Pharmacological inhibition of the vitronectin receptor abrogates PDGF-BB-induced hepatic stellate cell migration and activation in vitro. *J. Hepatol.* 2007, *46*, 878–887.

[37] Patsenker, E., Popov, Y., Stickel, F., Schneider, V. et al., Pharmacological inhibition of integrin alphavbeta3 aggravates experimental liver fibrosis and suppresses hepatic angiogenesis. *Hepatology* 2009, *50*, 1501–1511.

[38] Edwards, S., Lalor, P. F., Tuncer, C., Adams, D. H., Vitronectin in human hepatic tumours contributes to the recruitment of lymphocytes in an alpha v beta3-independent manner. *Br. J. Cancer* 2006, *95*, 1545–1554.

[39] Furutani, T., Hino, K., Okuda, M., Gondo, T. et al., Hepatic iron overload induces hepatocellular carcinoma in transgenic mice expressing the hepatitis C virus polyprotein. *Gastroenterology* 2006, *130*, 2087–2098.

[40] Nishina, S., Korenaga, M., Hidaka, I., Shinozaki, A. et al., Hepatitis C virus protein and iron overload induce hepatic steatosis through the unfolded protein response in mice. *Liver. Int.* 2010, *30*, 683–692.

[41] Franchini, M., Targher, G., Capra, F., Montagnana, M., Lippi, G., The effect of iron depletion on chronic hepatitis C virus infection. *Hepatol. Int.* 2008, *2*, 335–340.

